Multi-actuated Functionally Graded Piezoelectric Micro-Tools Design Using Topology Optimization

Ronny C. Carbonari[a], Emílio C. N. Silva[a], and Glaucio H. Paulino[b]

[a]Department of Mechatronics ad Mechanical Systems Engineering
Escola Politécnica da Universidade de São Paulo
Av. Prof. Mello Moraes, 2231, São Paulo - SP - 05508-900, Brazil
[b]Department of Civil and Environmental Engineering,
University of Illinois at Urbana-Champaign,
Newmark Laboratory, 205 North Mathews Av., Urbana, IL, 61801, USA.

ABSTRACT

The micro-tools considered in this work consist essentially of multi-flexible structures actuated by two or more piezoceramic devices that must generate different output displacements and forces at different specified points of the domain and on different directions. The multiflexible structure acts as a mechanical transformer by amplifying and changing the direction of the piezoceramics output displacements. Micro-tools offer significant promise in a wide range of applications such as cell manipulation, microsurgery, and micro/nanotechnology processes. Although the design of these micro-tools is complicated due to the coupling among movements generated by various piezoceramics, it can be realized by means of topology optimization concepts. Recently, the concept of functionally graded materials (FGMs) has been explored in piezoelectric materials to improve performance and increase lifetime of piezoelectric actuators. Usually for an FGM piezoceramic, elastic, piezoelectric, and dielectric properties are graded along the thickness. Thus, the objective of this work is to study the influence of piezoceramic property gradation in the design of the multiflexible structures of piezoelectric micro-tools using topology optimization. The optimization problem is posed as the design of a flexible structure that maximizes different output displacements or output forces in different specified directions and points of the domain, in response to different excited piezoceramic portions: while minimizing the effects of movement coupling. The method is implemented based on the solid isotropic material with penalization (SIMP) model where fictitious densities are interpolated in each finite element, providing a continuum material distribution in the domain. As examples, designs of a single piezoactuator and an XY nano-positioner actuated by two FGM piezoceramics are considered. The resulting designs are compared with designs considering homogeneous piezoceramics. The present examples are limited to two-dimensional models because most of the applications for such micro-tools are planar devices.

Keywords: Micro-/nano-positioners, MEMS, FGM, piezoelectric actuators, topology optimization, finite element analysis

1. INTRODUCTION

Micro-tools offer significant promise in a wide range of applications such as cell manipulation, microsurgery, and micro/nanotechnology processes.[1–3] The micro-tools considered in this work essentially consist of multi-flexible structures actuated by two or more FGM ("Functionally Graded Material") piezoceramic devices that must generate different output displacements and forces at different specified points of the domain and on different directions (see Figure 1). The multiflexible structure acts as a *mechanical transformer* by amplifying and changing the direction of the piezoceramics output displacements.[4] Thus, the development of these piezoelectric micro-tools requires the design of actuated compliant mechanisms[5] that can perform detailed specific movements.

Further author information:
Ronny C. Carbonari: E-mail: ronny@usp.br, Telephone: +55 (11) 3091 9851
Emílio C. N. Silva: E-mail: ecnsilva@usp.br, Telephone: +55 (11) 3091 9754
Glaucio H. Paulino: E-mail: paulino@uiuc.edu, Telephone: +1 (217) 333 3817

Smart Structures and Materials 2006: Modeling, Signal Processing, and Control,
edited by Douglas K. Lindner, Proc. of SPIE Vol. 6166, 616609, (2006)
0277-786X/06/$15 · doi: 10.1117/12.658503

Although the design of these micro-tools is complicated due to the coupling between movements generated by various piezoceramics, it can be realized by means of the topology optimization method.[6]

FGMs are advanced materials that possess continuously graded properties and are characterized by spatially varying microstructures created by nonuniform distributions of the reinforcement phase as well as by interchanging the role of reinforcement and matrix (base) materials in a continuous manner.[7] The smooth variation of properties may offer advantages such as local reduction of stress concentration and increased bonding strength. Recently, the concept of FGMs has been explored in piezoelectric materials to improve the properties and increase the lifetime of piezoelectric actuators.[8] Usually in an FGM piezoceramic, elastic, piezoelectric, and dielectric properties are graded along the thickness. Previous studies[8,9] have shown that the gradation law of piezoceramic properties can influence the performance of piezoactuators, such as generated output displacements. This suggests that optimization techniques can be applied to take advantage of the property gradation variation to improve the FGM piezoactuator. Figure 1 illustrates the concept of multi-actuated flextensional piezoelectric devices.

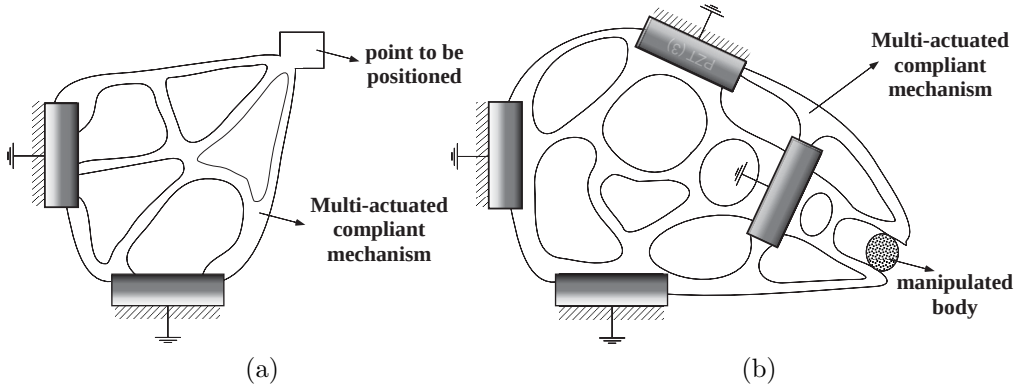

Figure 1. Concept of multi-actuated flextensional FGM piezoelectric devices. (a)XY nanopositioner; (b) Piezoceramics are responsible for XY displacements, rotation, and open/close movement of jaw.

The objective of this work is to study the influence of the piezoceramic property gradation variation in the design of multiflexible structures of piezoelectric micro-tools using topology optimization. The optimization problem is posed as the design of a flexible structure, as well as, each piezoceramic property gradation variation, that maximizes different output displacements or output forces in different specified directions and points of the domain, in response to different excited piezoceramic portions, while minimizing the effects of movement coupling. The method is implemented based on the solid isotropic material with penalization (SIMP) model where fictitious densities are interpolated at each finite element, providing a continuous material distribution in the domain. As examples, design of a single piezoactuator and an XY nano-positioner actuated by two FGM piezoceramics are considered. The resulting design is compared with design considering homogeneous piezoceramics.

2. FINITE ELEMENT FGM PIEZOELECTRIC MODELING

The micro-tools considered here operate in quasi-static or low-frequency (inertia effects are neglected). The linear finite element method (FEM) matrix formulation of the equilibrium equations for the piezoelectric medium is given by[10]:

$$\begin{bmatrix} \mathbf{K_{uu}} & \mathbf{K_{u\phi}} \\ \mathbf{K}^t_{\mathbf{u}\phi} & -\mathbf{K}_{\phi\phi} \end{bmatrix} \begin{Bmatrix} \mathbf{U} \\ \mathbf{\Phi} \end{Bmatrix} = \begin{Bmatrix} \mathbf{F} \\ \mathbf{Q} \end{Bmatrix} \Longrightarrow [\mathcal{K}]\{\mathcal{U}\} = \{\mathcal{Q}\} \tag{1}$$

where $\mathbf{K_{uu}}$, $\mathbf{K_{u\phi}}$, and $\mathbf{K}_{\phi\phi}$ are the stiffness, piezoelectric, and dielectric matrices, respectively, and $\mathbf{F}$, $\mathbf{Q}$, $\mathbf{U}$, and $\mathbf{\Phi}$ are the nodal mechanical force, nodal electrical charge, nodal displacements, and nodal electric potential vectors, respectively.[10]

In the case of FGM piezoceramics, all properties change continuously inside the piezoceramic domain, which means that they can be described by some continuous function of position ($\mathbf{x}$) in the piezoceramic domain, that is:

$$\mathbf{c}^E = \mathbf{c}^E(\mathbf{x});\ \mathbf{e} = \mathbf{e}(\mathbf{x});\ \boldsymbol{\epsilon}^S = \boldsymbol{\epsilon}^S(\mathbf{x}) \tag{2}$$

where $\mathbf{c}^E$, $\mathbf{e}$, and $\boldsymbol{\epsilon}^S$ denote the stiffness, piezoelectric and dielectric properties, respectively. From the mathematical definitions of $\mathbf{K_{uu}}$, $\mathbf{K_{u\phi}}$, and $\mathbf{K}_{\phi\phi}$, these material properties remain inside the matrices integrals and are integrated using the graded finite element concept[11] where properties are continuously interpolated inside each finite element based on property values at each finite element node. Approximation of the continuous change of material properties by a stepwise function, where a property value is assigned for each finite element, results in undesirable discontinuity of the stress field.[11]

When a non-piezoelectric conductor material and a piezoceramic material are distributed in the piezoceramic domain, the electrode positions are not known "a priori", as discussed in Section 4. Thus, the electrical excitation will be given by an applied electric field.[12] In this case, all electrical degrees of freedom are prescribed in the FEM problem, and thus Eq. (1) becomes:

$$\begin{bmatrix} \mathbf{K_{uu}} & \mathbf{K_{u\phi}} \\ \mathbf{K}^t_{\mathbf{u}\phi} & -\mathbf{K}_{\phi\phi} \end{bmatrix} \begin{Bmatrix} \mathbf{U} \\ \mathbf{\Phi} \end{Bmatrix} = \begin{Bmatrix} \mathbf{F} \\ \mathbf{Q} \end{Bmatrix} \Longrightarrow \begin{cases} [\mathbf{K_{uu}}]\{\mathbf{U}\} = \{\mathbf{F}\} - [\mathbf{K_{u\phi}}]\{\mathbf{\Phi}\} \\ \left[\mathbf{K}^t_{\mathbf{u}\phi}\right]\{\mathbf{U}\} = \{\mathbf{Q}\} + [\mathbf{K}_{\phi\phi}]\{\mathbf{\Phi}\} \end{cases} \tag{3}$$

where $\{\mathbf{\Phi}\}$ is prescribed. Thus, the mechanical and electrical problems are decoupled, and only the upper problem of Eq. (3) needs to be directly solved. Essentially, the optimization problem will be based on the mechanical problem. As a consequence, the dielectric properties will not influence the design.

3. DESIGN PROBLEM FORMULATION

The topology optimization formulation used in this work is described in detail by Carbonari *et al.*[6] and it is based on the continuous topology optimization concept in which a continuous distribution of the design variable inside the finite element is considered through interpolation using a continuous function. In this case, the design variables are defined for each element node, instead of each finite element as usual. This formulation, known as CAMD ("Continuous Approximation of Material Distribution")[13,14] appears more robust for designing piezoelectric micro-tools.[6] The material model is based on the SIMP ("Solid Isotropic Material with Penalization")[15] method combined with the CAMD approach, and states that at each point of the domain, the local effective stiffness of the mixture $\mathbf{C}^H$ as

$$\mathbf{C}^H = \rho_1^p \mathbf{C_0} \tag{4}$$

where $\mathbf{C}^H$ and $\mathbf{C_0}$ are the Young's modulus of the homogenized material and basic material that will be distributed in the domain, respectively, ρ_1 is a pseudo-density describing the amount of material at each point of the design domain, which can assume values between 0 and 1, and $p \in [1,4]$ is a penalization factor to recover the discrete design. For ρ_1 equal to 0 the material is equal to void, and for ρ_1 equal to 1 the material is equal to solid material. For a discretized domain into finite elements with continuous distribution of design variable, Eq. (4) is considered for each element node, and the material property (e.g. Young's modulus) inside each finite element is given by a function $\rho_1(\mathbf{x})$. This formulation allows a continuous distribution of material along the design domain, instead of the traditional piecewise material distribution applied to previous formulations of topology optimization, and it is ideal for the FGMs considered in the piezoceramic domain.

Because the objective is also to optimize the material gradation in the piezoceramic domain, an additional material model must be defined for the domain. In this work, the following material model is proposed based on an simple extension of the traditional SIMP:

$$\mathbf{C}^H = \rho_2 \mathbf{C_1} + (1-\rho_2)\mathbf{C_2} \tag{5}$$

$$\mathbf{e}^H = \rho_2 \mathbf{e_1} + (1-\rho_2)\mathbf{e_2} \tag{6}$$

where ρ_2 ($\rho_2 = 1.0$ denotes piezoelectric material **type 1** or $\rho_2 = 0.0$ denotes piezoelectric material **type 2**) refers to the pseudo-density function describing the amount of material at each point of the domain. The design variables can assume different values at each finite element node. $\mathbf{C}^H$ and $\mathbf{e}^H$ are stiffness and piezoelectric tensor properties, respectively, of the homogenized material. $\mathbf{C_1}$ and $\mathbf{e}_1$ are tensors related to the stiffness and piezoelectric properties for piezoelectric material **type 1**, respectively; and, similarly, $\mathbf{C_2}$ and $\mathbf{e_2}$ refer to the piezoelectric material **type 2**. These are the properties of basic materials that will be distributed in the piezoceramic domain to form the FGM composite. The dielectric properties are not considered because a constant electric field is applied to the design domain as electrical excitation. As explained in Section 2, this decouples the electrical and mechanical problems eliminating the influence of dielectric properties in the optimization problem. Eventually, the piezoelectric material **type 2** can be substituted by the flexible structure material (non-piezoelectric material, such as Aluminum, for example), and in this case $\mathbf{e_2} = \mathbf{0}$. Analogous to the material model described by Eq. (4), ρ_2 does have a continuous distribution along the piezoceramic design domain, that is, $\rho_2 = \rho_2(\mathbf{x})$, and so do the material properties. For a discretized domain into finite elements, ρ_2 and Eqs. (5) and (6) are considered for each finite element node. Thus, by finding the nodal values of the unknown ρ_2 function, we obtain indirectly the optimum material distribution functions, described by Eq. (2).

The theoretical formulation for piezoelectric micro-tool design problem by using topology optimization was developed by Carbonari *et al.*[6] and it is briefly presented here. Essentially, a piezoelectric multi-actuator consists of a coupling structure actuated by two or more piezoceramics[4] where each piezoceramic is responsible for actuating a specific multi-actuator movement. In addition, there is a coupling among actuated displacements due to the fact that it is a flexible structure.[5] When a piezoceramic is excited to generate a desired displacement, other undesired displacements are generated. This generated undesired displacements can be decreased by decoupling at most the actuated and undesired displacements. Figure 2 shows an example of a coupling structure multi-actuated by piezoceramics.

Regarding the electrical excitation, when the distribution of a non-piezoelectric conductor material (such as Aluminum, for example) and a piezoceramic material is considered in the piezoceramic domain, the electrode positions are not known "a priori". To circunvent this problem an electric field is applied as electrical excitation.[12] When two piezoelectric materials are considered, the electrode positions are known and an electric field excitation can be achieved by applying an electric voltage to the electrodes.

Therefore, in the formulation of the piezoelectric multi-actuator design optimization the objective is to design a device such that when each piezoceramic is actuated, it generates an output displacement in a specified point and direction with minimum coupling with displacements generated by other piezoceramics in other points and directions. Thus, this design problem is related to flexible structures design theory considering multi-flexibility.[16] The objective function is defined in terms of a combination of output displacements generated for a specified applied electric field to each piezoceramic, and it must also minimize the coupling among displacements, which can be achieved by including coupling constraints.[6]

Considering a specific actuation movement i, the mean transduction, or electromechanical function ($L_2^i(\mathbf{u}_1^i, \phi_1^i)$) is related to the output displacement generated due to the applied electric field (see Figure 2). In the notation $L_j^i(\mathbf{u}_k^i, \phi_k^i)$ the indices i, j, and k refer to the piezoceramic number, dummy load case, and considered load case, respectively. $\mathbf{u}$ and ϕ are the displacement and electric field, respectively.[6] To provide some stiffness to the multi-flexible structure the mean compliance $L_3^i(\ \mathbf{u}_3^i, \phi_3^i)$ must also be minimized. The coupling constraint is obtained by minimizing the absolute value of the corresponding mean transduction $L_4^i(\mathbf{u}_1^i, \phi_1^i)$ between actuated piezoceramic and generated undesired displacement. Finally, a multi-objective function which properly combines these three functions is constructed to find an appropriate optimal solution that can incorporate all design requirements, considering actuation movement i. The optimization problem has a volume constraint of material in the design domain, and we refer to Carbonari *et al.*[6] for more details.

In the design of the multi-actuated FGM piezoelectric micro-tools, an extra optimization problem of the same type is solved for the piezoceramic domain to find the optimum gradation of the piezoelectric material, however, the optimization will have the nodal values of $\rho_2(\mathbf{x})$ as design variables.

The final optimization problem is defined as:

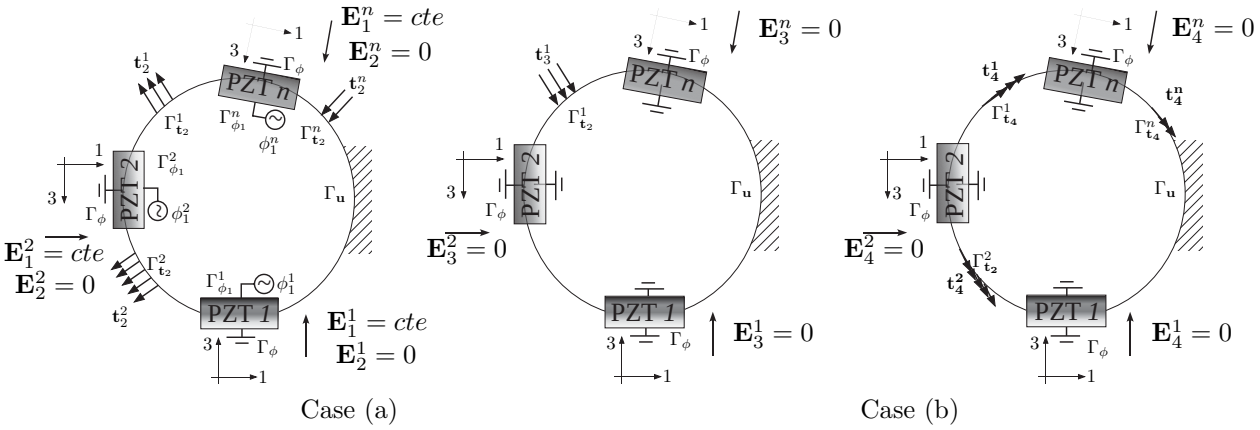

Figure 2. Coupling structure multi-actuated by FGM piezoceramics. Load cases for calculation of: mean transduction and coupling constraint (case (a)), mean compliance (case (b)) (only for piezoceramic "1"). Here, $\mathbf{E}_i^j = -\nabla\phi_i$ denotes the electrical field associated with load case i applied to piezoceramic "j".

$$
\begin{aligned}
&Maximize: && \mathcal{F}(\rho_1,\rho_2)\\
&\rho_1,\rho_2 &&\\
&subject\ to: && \text{Equilibrium equations for different load cases}\\
& && 0 \le \rho_1 \le 1,\ 0 \le \rho_2 \le 1\\
& && \Theta_1(\rho) = \textstyle\int_S \rho_1 dS - \Theta_{1S} \le 0\\
& && \Theta_2(\rho) = \textstyle\int_{S_{PZT}} \rho_2 dS - \Theta_{2S} \le 0
\end{aligned}
$$

where $\mathcal{F}(\rho_1,\rho_2)$ is a multi-objective function defined as a function of mean transduction and mean compliance functions in the problem as described in detail by Carbonari *et al.*.[6] S is the design domain Ω without including the piezoceramic, Θ_1 is the volume of this design domain, and Θ_{1S} is an upper-bound volume constraint defined to limit the maximum amount of material used to build the coupling structure. S_{PZT} is the piezoceramic domain, Θ_2 is the volume related to ρ_2 design variable, and Θ_{2S} is an upper-bound volume constraint defined to limit ρ_2 values when optimizing the FGM gradation function. The other constraints are equilibrium equations for piezoelectric medium considering different load cases. The equilibrium equations are solved separately from the optimization problem. They are stated in the problem to indicate that, whatever topology is obtained, it must satisfy the equilibrium equations. Our notation follows the work of Bendsøe and Kikuchi.[17]

4. NUMERICAL IMPLEMENTATION

The continuous distribution of design variables $\rho_1(\mathbf{x})$ and $\rho_2(\mathbf{x})$ are given by the functions[13,14]

$$\rho_1(\mathbf{x}) = \sum_{I=1}^{n_d} \rho_{1I} N_I(\mathbf{x});\ \rho_2(\mathbf{x}) = \sum_{I=1}^{n_d} \rho_{2I} N_I(\mathbf{x}) \tag{7}$$

where ρ_{1I} and ρ_{2I} are nodal design variables, N_I is the finite element shape function, and n_d is the number of nodes at each finite element. The design variables ρ_{1I} and ρ_{2I} can assume different values at each node of the finite element. Due to the definition of Eqs. 7, the material property functions (Eqs. 5 and 6) will also have a continuous distribution inside the design domain. Thus, considering the mathematical definitions of the stiffness and piezoelectric matrices of Eq. (1), the material properties must remain inside the integrals and be integrated together by means of the graded finite element concept.[11] The finite element equilibrium equation (1) is solved considering 4-node isoparametric finite elements under either a plane stress or plane strain assumption. The numerical expressions for mean transduction and mean compliance as a function of FEM matrices, described in Eq. (1), are provided in detail in references.[6,18]

When non-piezoelectric conductor material (usually metal, such as, Aluminum) is considered in Eqs. (5) and (6), a relevant problem to be solved is how to define the piezoceramic electrodes. If only different types of piezoelectric materials are considered in these equations, the position of electrodes surface is known and is defined by the piezoceramic domain geometry. However, if a non-piezoelectric conductor material (for example, Aluminum) is also distributed in the piezoceramic design domain, we cannot define "a priori" the position of the piezoceramic electrodes because we do not know where the piezoceramic is located in the design domain. To circunvent this problem, we consider the electrical problem independently for each finite element of the piezoceramic domain by defining a pair of electrodes at each finite element, that is, each finite element has its own electrical degrees of freedom as described in Figure 3.

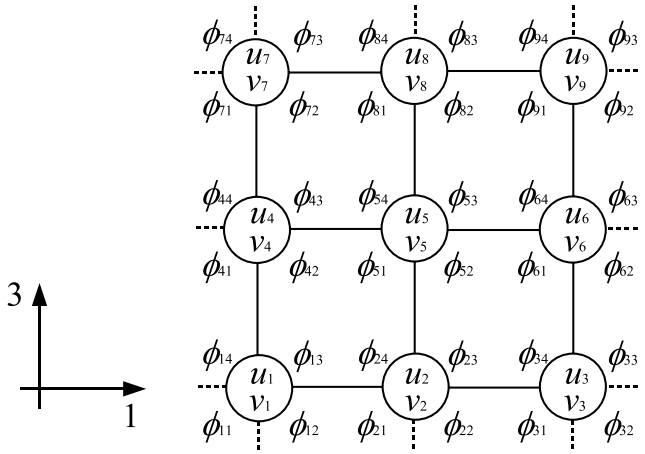

Figure 3. Finite elements with their corresponding electrical degrees of freedom. The notation is defined as follows, u_i and v_i denote the node i horizontal and vertical displacement, respectively, and ϕ_{ij} denotes the j-th potential at the i-th node.

Thus, each finite element has 4 electrical degrees of freedom given by $[\phi_a, \phi_b, \phi_c, \phi_d]$ (nodes are ordered counterclockwise starting from the upper right corner of each finite element) considering that one of the electrodes is grounded. Electrical voltage ϕ_0 is applied to the two upper nodes, and thus, the four electrical degrees of freedom are prescribed at each finite element, as follows ($[\phi_0, \phi_0, 0, 0]$).[12] This is equivalent to applying a constant electrical field along the 3-direction in the design domain (see Figure 3). In this case, all electrical degrees of freedom are prescribed in the FEM problem, as already mentioned in Section 2.

The discretized form of the optimization problem is stated as:

$$
\begin{array}{lll}
Maximize: & \mathcal{F}\left(\rho_{1I}, \rho_{2J}\right) & \\
\rho_{1I},\ \rho_{2J} & & \\
subject\ to: & \text{Equilibrium equations for different load cases} & \\
 & 0 \leq \rho_{1I} \leq 1;\ 0 \leq \rho_{2J} \leq 1 & I = 1..N_e; J = 1..N_p \\
 & \sum_{I=1}^{N_e} \rho_{1I} V_I - \Theta_{1S} \leq 0 & \\
 & \sum_{I=1}^{N_p} \rho_{2I} V_I - \Theta_{2S} \leq 0 &
\end{array}
$$

where V_I is the volume associated with each finite element node, which is equal to finite element volume; and N_e is the number of nodes in the non-piezoceramic design domain and N_p is the number of nodes in the piezoceramic design domain .

The boundary conditions for the piezoceramic domain for load cases (a) and (b) of Figure 2 are shown in Figures 4(a) and (b), respectively. They represent constant and null electric field, respectively, applied to the domain.

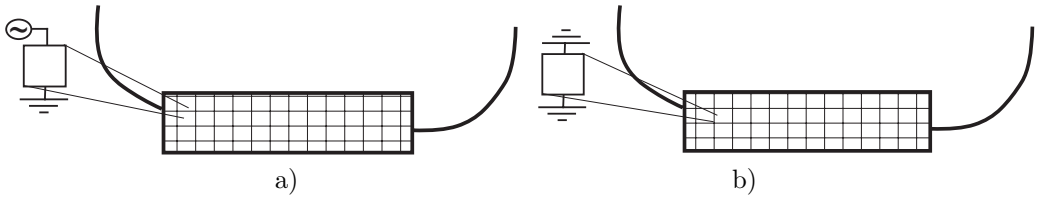

Figure 4. Boundary conditions for the piezoceramic domain: (a)mean transduction and coupling constraint function ($\nabla\phi = cte.$); (b)mean compliance ($\nabla\phi = 0$).

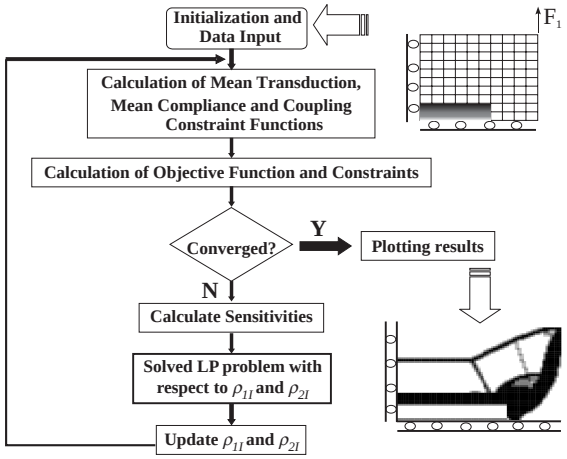

Figure 5. Flow chart of optimization procedure.

A flow chart of the optimization algorithm describing the steps involved is shown in Figure (5). The software was implemented using the C language.

The mathematical programming method called Sequential Linear Programming (SLP) is applied to solve the optimization problem since there are a large number of design variables, and different objective functions and constraints.[18–20] The linearization of the problem at each iteration requires the sensitivities (gradients) of the multi-objective function and constraints. These sensitivities will depend on gradients of mean transduction and mean compliance functions in relation to ρ_{1I} and ρ_{2J}. The derivations are given by Carbonari *et al.*.[6]

Suitable moving limits are introduced to assure that the design variables do not change by more than 5–15% between consecutive iterations. A new set of design variables ρ_{1I} and ρ_{2J} are obtained after each iteration, and the optimization continues until convergence is achieved for the objective function. The results are obtained using the continuation method where the penalization coefficient p varies from 1 to 4 along the iterations. The continuation method alleviates the problem of the multiple local minimum (or maximum).[15]

5. EXAMPLE AND RESULTS

5.1. Single Piezoactuator Design

Examples are presented to illustrate the design of piezoelectric micro-tools with FGM piezoceramics using the proposed method. The design domains used for the examples are shown in Figure 6. They consist of regions of piezoceramic whose shape remains unchanged during the optimization, and a domain S of Aluminum. The objectives of optimization are to find the optimum material property gradation variation in the piezoceramic domain, and the flexible structure optimum topology in the domain S. The piezoceramic design domain is divided in horizontal layers and a design variable (pseudo density ρ_{2J}) is considered for each layer interface as described in Figure 7.

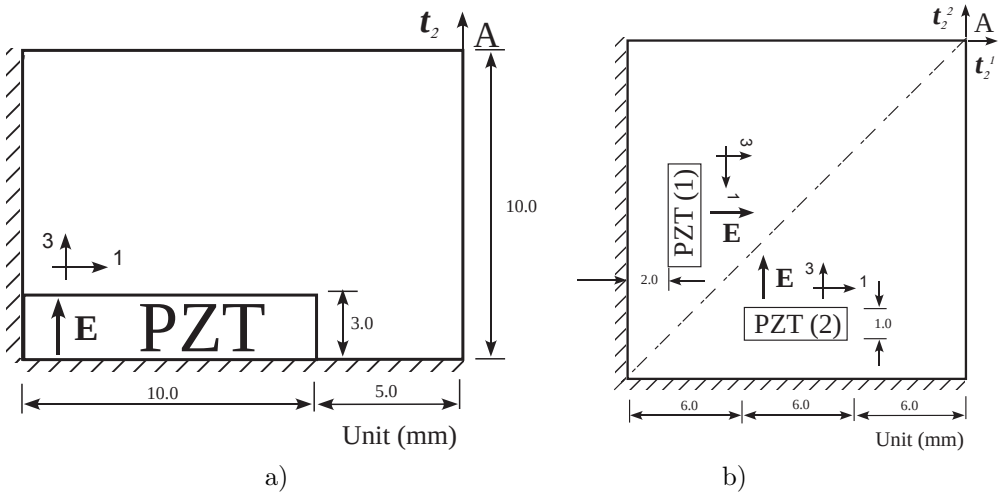

Figure 6. Design domains: (a) single piezoactuator; (b) XY piezoelectric nanopositioner.

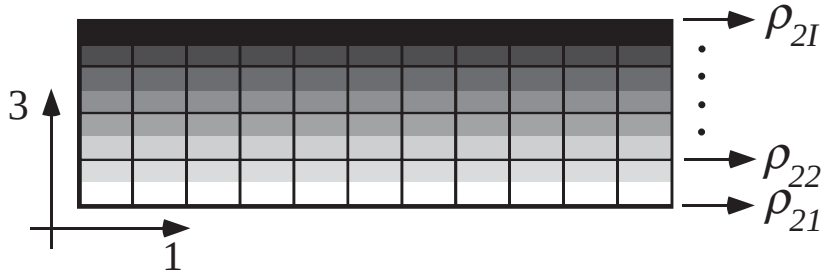

Figure 7. Piezoceramic design domain divided in horizontal layers. A design variable is defined for each layer interface.

Table (1) presents the piezoelectric material properties used in the simulations for all examples. Here, $\mathbf{c}^E$ and $\mathbf{e}$ are the elastic and piezoelectric properties of the medium, respectively. The Young's modulus and Poisson's ratio of Aluminum are equal to 70 GPa and 0.33, respectively. Two-dimensional isoparametric finite elements under plane-stress assumption are used in the finite element analysis.

Table 1. Material Properties of PZT5A.

c_{11}^E (10^{10} N/m^2)	12.1	e_{13} (C/m^2)	-5.4
c_{12}^E (10^{10} N/m^2)	7.54	e_{33} (C/m^2)	15.8
c_{13}^E (10^{10} N/m^2)	7.52	e_{15} (C/m^2)	12.3
c_{33}^E (10^{10} N/m^2)	11.1		
c_{44}^E (10^{10} N/m^2)	2.30		
c_{66}^E (10^{10} N/m^2)	2.10		

The amount of electric field applied to any of the piezoceramics is 2000 V/mm (see Figure 6). For all examples, the value of w coefficient is equal to 0.5. Values of other optimization parameters not described here are adopted equal to the values presented by Carbonari *et al.*.[6] The initial values of design variables (ρ_{1I} and ρ_{2J}) are set equal to 0.15. The optimization problem starts in the feasible domain (all constraints satisfied). The designs are shown by plotting the average density value.

In the first example, the design of a single type piezoactuator is considered and the influence of the displace-

ment coupling constraint is shown. The design domain for this problem is shown in Figure 6(a) and it has 3750 finite elements (rectangle discretized by a 75×50 mesh). The piezoceramic domain was discretized into 15 layers, thus, 16 design variables. The mechanical and electrical boundary conditions are shown in Figure 6(a). The volume constraint Θ_{1S} is equal to 25% of the volume of the whole domain Ω without piezoceramic domain, the volume constraint of the piezoceramic material Θ_{2S} is equal to 50%. The piezoactuator is designed by both taking and not taking into account the displacement coupling constraint function. Thus, the topology optimization problem is solved considering coefficient β equal to 0.0 and 0.1, respectively. The topology optimization results are shown in Figure 8.

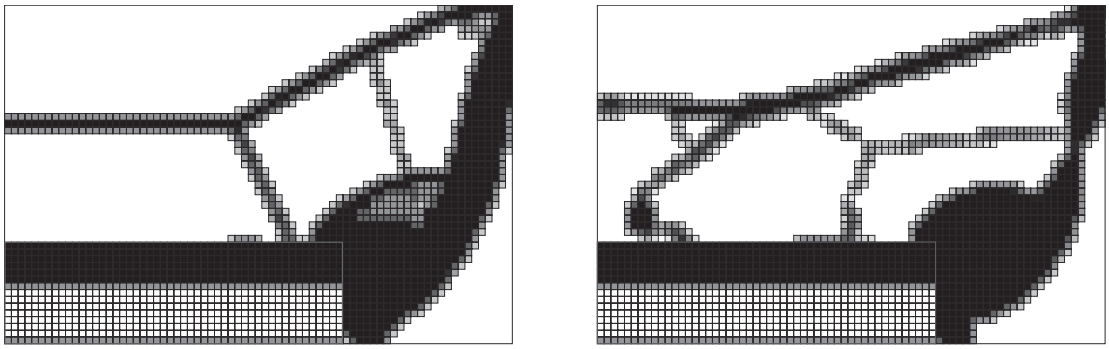

a) b)

Figure 8. Optimal topology results considering the influence of displacement coupling constraint; (a) $\beta = 0.0$; (b) $\beta = 0.1$.

In both designs, the optimization finished with the constraint Θ_2 active, which means that half of the piezoceramic domain is made of piezoceramic material. Table 2 describes X and Y displacements at point A (u_x and u_y) (see Figure 8(a)) considering $2000V/mm$ electric field applied to the piezoceramic and coupling factors ($R_{yx} = u_x/u_y$) for the piezoactuator designs. It is noticed that the displacement coupling is reduced when the coupling constraint function is activated, however, this decrease is due to a change in the coupling structure topology rather than the piezoceramic property gradation variation. In addition, the generated displacement is decreased with the increase of β as already noticed by Carbonari *et al.*.[6]

Table 2. Vertical displacement at point A and coupling factor ($R_{yx} = u_x/u_y$).

Piezoactuators	$u_x(n\text{m})$	$u_y(n\text{m})$	$R_{yx}(\%)$	w	β
Fig.8a	425.12	-409.94	96.4	0.5	0.0
Fig.8b	431.64	-172.90	40.1	0.5	0.1
Fig.9a	505.3	-183.4	36.3	0.5	0.0
Fig.9b	446.8	-169.4	37.9	0.5	0.0

5.2. XY Piezoelectric Nanopositioner

In the second example, the design of a XY piezoelectric nanopositioner is considered and the influence of piezoceramic property gradation variation is analyzed in the design. The design domain for this problem is symmetric and it has two piezoceramic domains as shown in Figure 6(b). The FEM discretization consists of 8100 finite elements (rectangle discretized by a 90×90 mesh). Each piezoceramic domain is discretized into 5 layers, thus, 6 design variables, with a total of 12 design variables. The mechanical and electrical boundary conditions are shown in Figure 6(b). Two XY nanopositioner designs were obtained. In both of them the volume constraint Θ_{1S} is equal to 25% of the volume of the whole domain Ω without piezoceramic domain, however, the volume constraint of the piezoceramic material Θ_{2S} is set equal to 100% and 50%, respectively. The displacement constraint function was not considered, thus, the coefficient β was set equal to zero for both

results. The penalization coefficient p was varied from 1 to 3 along the iterations. The topology optimization designs are shown in Figure 9.

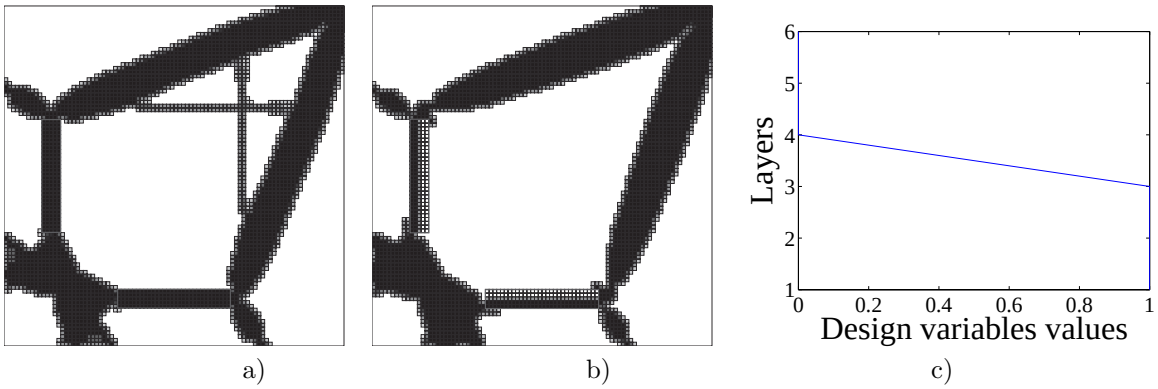

Figure 9. Optimal topology results considering the influence of piezoceramic property gradation variation; (a) $\Theta_{2S} = 100\%$; (b) $\Theta_{2S} = 50\%$; (c) ρ_{2I} distribution in piezoceramic domain for $\Theta_{2S} = 50\%$.

The optimization finished with the constraint Θ_2 active in both designs. The first result is equivalent to a design considering an homogeneous piezoceramic (non-FGM). Notice that the coupling structure topology is slightly changed. Table 2 describes X and Y displacements at point A (u_x and u_y) (see Figure 6(a)) considering $2000V/mm$ electric field applied to the piezoceramic and coupling factors (R_{yx}) for obtained nanopositioner designs. We conclude that even though the piezoceramics of the first nanopositioner (Figure 9(a)) has double amount of piezoelectric material with respect to the piezoceramics of second nanopositioner (Figure 9(b)), it generates a displacement only 13% larger. The displacement coupling was not changed.

6. CONCLUSIONS

The optimized design of piezoelectric micro-tools actuated by FGM piezoceramics is obtained by means of the topology optimization method. The coupling structure topology and the piezoceramic property gradation are simultaneously optimized. The designs are compared with these considering homogeneous piezoceramics (non-FGM) and the influence of using FGM piezoceramics is analyzed. Based on the results obtained, we conclude that almost the same values of displacement could be obtained, however smaller amount of piezoceramic are used by applying the FGM concept. The optimum topologies of coupling structures are also slightly changed when FGM piezoceramics are considered.

Acknowledgements

The first and second authors thank University of São Paulo (Brazil) and Fundação de Amparo à Pesquisa do Estado de São Paulo (FAPESP - Research Support Foundation of São Paulo State) for supporting them through a research project. The first author thanks the CNPq - Conselho Nacional de Desenvolvimento Científico e Tecnológico - Brazil, for supporting him through a doctoral fellowship ($n.^o 140687/2003-3$).

REFERENCES

1. H. Ishihara, F. Arai, and T. Fukuda, "Micro mechatronics and micro actuators," *IEEE/ASME Transactions on Mechatronics* **1**(1), pp. 68–79, 1996.
2. A. Menciassi, A. Eisinberg, M. C. Carrozza, and P. Dario, "Force sensing microinstrument for measuring tissue properties and pulse in microsurgery," *IEEE/ASME Transactions on Mechatronics* **8**(1), pp. 10–17, 2003.
3. A. Ferreira, J. Agnus, N. Chaillet, and J. M. Breguet, "A smart microrobot on chip: Design, identification, and control," *IEEE/ASME Transactions on Mechatronics* **9**(3), pp. 508–519, 2004.

4. F. Claeyssen, R. L. Letty, F. Barillot, N. Lhermet, H. Fabbro, P. Guay, M. Yorck, and P. Bouchilloux, "Mechanisms based on piezo actuators," in *Proceedings on Industrial and Commercial Applications of Smart Structures Technologies of* 8^{th} *SPIE (Annual International Symposium on Smart Structures and Materials)*, **4332**, pp. 225–233, 2001.
5. L. L. Howell, *Compliant Mechanisms*, John Wiley & Sons, Inc., New York, USA, 2001.
6. R. C. Carbonari, E. C. N. Silva, and S. Nishiwaki, "Design of piezoelectric multiactuated microtools using topology optimization," *Smart Materials and Structures* **14**, pp. 1431–1447, 2005.
7. S. Suresh and A. Mortensen, *Fundamentals of Functionally Graded Materials*, IOM Communications Ltd., London, England, 1988.
8. A. Almajid, M. Taya, and S. Hudnut, "Analysis of out-of-plane displacement and stress field in a piezocomposite plate with functionally graded microstructure," *International Journal of Solids and Structures* **38**(19), pp. 3377–3391, 2001.
9. S. Zhifei, "General solution of a density functionally gradient piezoelectric cantilever and its applications," *Smart materials and Structures* **11**, pp. 122–129, 2002.
10. R. Lerch, "Simulation of piezoelectric devices by two-and three-dimensional finite elements," *IEEE Transactions on Ultrasonics, Ferroelectrics and Frequency Control* **37**(2), pp. 233–247, 1990.
11. J. H. Kim and G. H. Paulino, "Isoparametric graded finite elements for nonhomogeneous isotropic and orthotropic materials," *ASME Journal of Applied Mechanics* **69**(4), pp. 502–514, 2002.
12. M. J. Buehler, B. Bettig, and G. G. Parker, "Topology optimization of smart structures using a homogenization approach," *Journal of Intelligent Material Systems and Structures* **15**(8), pp. 655–667, 2004.
13. K. Matsui and K. Terada, "Continuous approximation of material distribution for topology optimization," *International Journal for Numerical Methods in Engineering* **59**(14), pp. 1925–1944, 2004.
14. S. Rahmatalla and C. C. Swan, "A q4/q4 continuum structural topology optimization implementation," *Structural and Multidisciplinary Optimization* **27**, pp. 130–135, 2004.
15. M. P. Bendsøe and O. Sigmund, *Topology Optimization - Theory, Methods and Applications*, Springer, New York, EUA, 2003.
16. S. Nishiwaki, S. Min, J. Yoo, and N. Kikuchi, "Optimal structural design considering flexibility," *Computer Methods in Applied Mechanics and Engineering* **190**, pp. 4457–4504, 2001.
17. M. P. B. e and N. Kikuchi, "Generating optimal topologies in structural design using a homogenization method," *Computer Methods in Applied Mechanics and Engineering* **71**, pp. 197–224, 1988.
18. E. C. N. Silva, S. Nishiwaki, and N. Kikuchi, "Topology optimization design of flextensional actuators," *IEEE Transactions on Ultrasonics, Ferroelectrics and Frequency Control* **47**(3), pp. 657–671, 2000.
19. G. N. Vanderplaatz, *Numerical Optimization Techniques for Engineering Design: with Applications*, McGraw-Hill, New York, USA, 1984.
20. R. Hanson and K. Hiebert, *A Sparse Linear Programming Subprogram*, Sandia National Laboratories, Technical Report SAND81-0297, 1981.